Formation and Reactivity of (Tetraarylporphyrinato)rhodium(II) Monocarbonyls: Bent $Rh^{II}CO$ Complexes That React like Acyl Radicals

Bradford B. Wayland,* Alan E. Sherry, George Poszmik, and Andrew G. Bunn

Contribution from the Department of Chemistry, University of Pennsylvania, Philadelphia, Pennsylvania 19104-6323. *Received March 18, 1991*

Abstract: Reactions for a series of rhodium(II) porphyrins with CO are used in illustrating the use of ligand steric effects in both promoting and inhibiting CO coupling to form α-diketone complexes ((por)RhC(O)C(O)Rh(por)). [Tetrakis-(2,4,6-trimethylphenyl)porphyrinato]rhodium(II), (TMP)Rh•, reacts with CO to produce an equilibrium between a C–C-bonded diamagnetic dimer (TMP)RhC(O)C(O)Rh(TMP), with a small amount of a paramagnetic ($S = {}^1/_2$) monomer, (TMP)RhCO, but only the monocarbonyl complex is observed for the most sterically demanding porphyrin complex examined: [tetrakis-(2,4,6-triisopropylphenyl)porphyrinato]rhodium(II), (TTiPP)Rh•. EPR spectra for (TMP)$Rh^{13}CO$ and (TTiPP)$Rh^{13}CO$ display three distinct g transitions which indicate the presence of nonlinear RhCO units. (TMP)RhCO reacts like an acyl radical, as evidenced by dimerization through C–C bonding to form (TMP)RhC(O)C(O)Rh(TMP), reactions with $(Bu)_3SnH$ and H_2 that produce the formyl complex (TMP)RhCHO, and reaction with styrene to form (TMP)$RhC(O)CH_2CH(C_6H_5)$C-(O)Rh(TMP). Thermodynamic and activation parameters for the dimerization of (TMP)RhCO through C–C bonding provides an enthalpy profile for the carbon monoxide coupling reaction.

Introduction

Activation of CO is typically accomplished by binding with Lewis acid metal centers which promote 2-electron reactions with nucleophiles at the carbonyl carbon.[1] Reactions of CO with rhodium(II) porphyrins have recently illustrated an alternate approach to CO activation through the use of metalloradicals to induce 1-electron carbonyl reactions.[2,3] This behavior was first realized in the reactions of (octaethylporphyrinato)rhodium(II) dimer, $[(OEP)Rh]_2$, with CO that produce a dimetal ketone, (OEP)RhC(O)Rh(OEP),[2] which has precedent in the chemistry of Pd(I) and Pt(I) *A-frame* complexes,[4] and at higher CO pressures a dimetal α-diketone, (OEP)RhC(O)C(O)Rh(OEP),[3] which was without precedent.

This paper describes how sequential increases in porphyrin ligand steric requirements produce selectivity for CO reductive coupling (MC(O)C(O)M) and how further increases in the ligand steric effects inhibit the CO coupling and permit direct observation of 17-electron monocarbonyl complexes, (por)RhCO•. Kinetic and thermodynamic studies for the dimerization of the tetramesitylporphyrin derivative, (TMP)RhCO, to form (TMP)RhC-(O)C(O)Rh(TMP) provide information on the nature of the 17-electron monocarbonyl and on the CO reductive coupling reaction. The monocarbonyls, (por)RhCO, are found to have nonlinear RhCO fragments and to behave like acyl radicals in dimerizing through C–C bonding and in reactions with styrene and sources of hydrogen atoms.

Results

Reactions of Rhodium(II) Porphyrins with CO. $[(TXP)Rh]_2$. [Tetrakis(3,5-dimethylphenyl)porphyrinato]rhodium(II) occurs primarily as a dimer, $[(TXP)Rh]_2$ (**1**), with a weak Rh^{II}–Rh^{II} bond (~12 kcal mol^{-1}).[5] Benzene solutions of **1** exposed to relatively low pressures of CO ($P_{CO} < 0.3$ atm) provide ^1H NMR evidence for the presence of a CO adduct, dimetal ketone, and dimetal α-diketone species like that observed for the $[(OEP)Rh]_2$ system.[3] The α-diketone, (TXP)RhC(O)C(O)Rh(TXP) (**2**), is the predominant CO-containing species throughout the range of conditions studied (P_{CO} = 0.1–1.0 atm; T = 220–300 K).[6] At CO pressures greater than 0.4 atm ($T < 300$ K) **2** is the only ^1H NMR observable species present. ^1H NMR spectra of **2** in benzene have high-field pyrrole peak positions and high-field split patterns for the ortho phenyl hydrogens which are features previously associated with two-atom-bridged complexes of other rhodium tetraphenylporphyrin systems.[7] Toluene solutions of the ^{13}C derivative of **2** display an AA'XX' ^{13}C NMR spectrum centered at δ = 165.5 that is virtually identical to that observed for (OEP)-RhC(O)C(O)Rh(OEP) (δ = 165.7).[3] Solvent sublimation from a frozen benzene solution of **2** (263 K) results in isolation of a yellow-orange solid which has two IR-active carbonyl stretching frequencies ($\nu_{^{12}CO}$ = 1778, 1767 cm^{-1}; $\nu_{^{13}CO}$ = 1738, 1727 cm^{-1}).

(TMP)Rh•. The steric requirements of tetramesitylporphyrin preclude dimerization of (TMP)Rh• through Rh–Rh boonding and provide a stable monomeric Rh^{II} complex, (TMP)Rh• (**3**).[8] EPR spectra for **3** in toluene glass (90 K) ($g_\perp$ = 2.65; $g_\parallel$ = 1.915) indicate that this low-spin d^7 ($S = {}^1/_2$) complex has a $(d_{xz}d_{yz}d_{xy})^6d_{z^2}{}^1$ electron configuration.[8]

Exposure of toluene solutions of (TMP)Rh• (**3**) to CO (P_{CO} ~ 0.1–1.0 atm; T = 260–300 K) results in appearance of an isotropic EPR spectrum for an $S = {}^1/_2$ species ($\langle g \rangle$ = 2.101). Repeating this experiment with ^{13}CO yields a doublet EPR spectrum associated with an isotropic ^{13}C hyperfine coupling constant of 313 MHz (296 K), and the spectrum in toluene glass (90 K) has a g_3 transition (g_3 = 1.995) that is a doublet of doublets due to ^{103}Rh ($A(^{103}Rh_{(g_3)})$ = 67 MHz) and ^{13}C hyperfine couplings ($A(^{13}C_{(g_3)})$ = 302 MHz) associated with the monocarbonyl complex, (TMP)RhCO (**4**) (Figure 1; eq 1). The EPR spectrum for

$$(TMP)Rh^{\bullet} + CO \rightleftharpoons (TMP)RhCO \qquad (1)$$

(TMP)$Rh^{13}CO$ in methylcyclohexane glass (90 K) shows three distinct g and $A(^{13}C)$ values: g_1 = 2.176, $A(^{13}C_{(g_1)})$ = 310 ± 3 MHz; g_2 = 2.147, $A(^{13}C_{(g_2)})$ = 327 ± 2 MHz; g_3 = 1.998, $A(^{13}C_{(g_3)})$ = 302 ± 2 MHz (Figure 2).

Formation of **4**, which is observed by EPR, is accompanied by the appearance of a diamagnetic species **5** that is observed by ^1H

(1) Ford, P. C.; Rokicki, A. *Adv. Organomet. Chem.* **1988**, *28*, 139.
(2) Wayland, B. B.; Woods, B. A.; Coffin, V. L. *Organometallics* **1986**, *5*, 1059–1062.
(3) Coffin, V. L.; Brennen, W.; Wayland, B. B. *J. Am. Chem. Soc.* **1988**, *110*, 6063–6069.
(4) (a) Cowie, M.; Southern, T. G. *J. Organomet. Chem.* **1980**, *193*, C46. Cowie, M.; Dwight, S. K. *Inorg. Chem.* **1980**, *19*, 2500. (b) Colton, R.; McCormick, M. J.; Pannan, C. D. *Aust. J. Chem.* **1978**, *32*, 1425. (c) Brown, M. P.; Puddephatt, R. J.; Rashidi, M.; Seddon, K. R. *J. Chem. Soc., Dalton Trans.* **1978**, 1540. Brown, M. P.; Keith, A. N.; Manojlovic-Muir, L.; Muir, K. W.; Puddephatt, R. J.; Seddon, K. R. *Inorg. Chim. Acta* **1979**, *34*, L223. (d) Kubiak, C. P.; Woodcock, C.; Eisenberg, R. *Inorg. Chem.* **1982**, *21*, 2119; *J. Am. Chem. Soc.* **1980**, *102*, 8637.
(5) Wayland, B. B.; Ba, S.; Sherry, A. E. *J. Am. Chem. Soc.* **1991**, *113*, 5305.
(6) Wayland, B. B.; Sherry, A. E.; Coffin, V. L. *J. Chem. Soc., Chem. Commun.* **1989**, 662.
(7) Wayland, B. B.; Van Voorhees, S. L.; Wilker, C. *Inorg. Chem.* **1986**, *25*, 4039.
(8) Sherry, A. E.; Wayland, B. B. *J. Am. Chem. Soc.* **1989**, *111*, 5010.

0002-7863/92/1514-1673$03.00/0

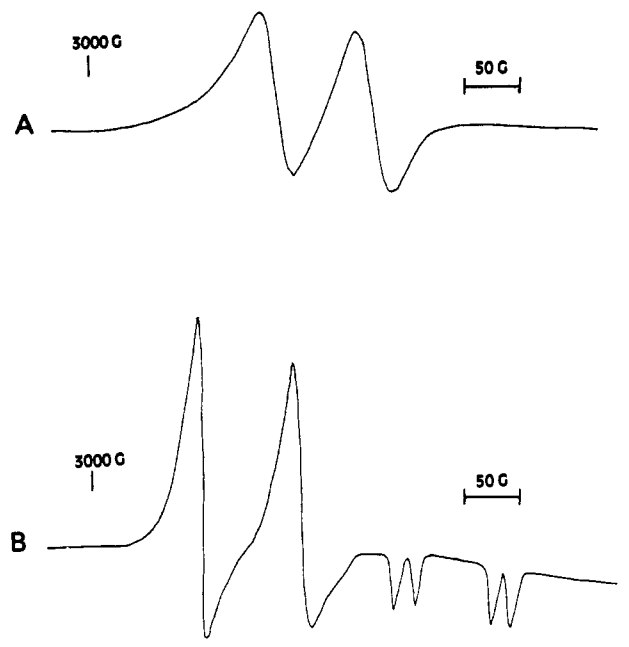

Figure 1. EPR spectra for (TMP)Rh^{13}CO in toluene (P_{CO} = 0.6 atm): (A) solution (296 K) ($\langle g \rangle$ = 2.101; $\langle A(^{13}C) \rangle$ = 313 MHz); (B) glass (90 K) (g_3 = 1.995; $A(^{13}C_{(g_3)})$ = 302 MHz; $A(^{103}Rh_{(g_3)})$ = 67 MHz).

and ^{13}C NMR. Compound **5** in toluene (193 K) displays an AA'XX' ^{13}C NMR pattern resulting from pairs of chemically equivalent but magnetically inequivalent ^{13}C and ^{103}Rh nuclei that is closely related to the spectra for α-diketone complexes of (OEP)Rh[3] and (TXP)Rh[6] which identifies this species as the C–C-bonded dimer of **4**, (TMP)RhC(O)C(O)Rh(TMP) (**5**) (eq 2). No evidence was found in the (TMP)Rh system for a dimetal ketone complex.

$$2(TMP)RhCO \rightleftharpoons (TMP)RhC(O)C(O)Rh(TMP) \quad (2)$$

Solvent sublimation at 260 K from a frozen benzene solution of **5** produces a solid which, as the Nujol mull, displays two transient bands in the CO stretching region ($\nu_{CO} \sim$ 1782, 1770 cm^{-1}). The two ν_{CO} bands decline in intensity and disappear as a set over a period of hours. Application of the same procedure for (TXP)RhC(O)C(O)Rh(TXP) (TXP = tetrakis(3,5-dimethylphenyl)porphyrin) and the ^{13}CO derivative results in a metastable solid with two CO stretching frequencies (ν_{12CO} = 1778, 1767 cm^{-1}, ν_{13CO} = 1738, 1727 cm^{-1}), which decline in intensity and disappear over a period of several days. Efforts to obtain solution spectra have not yet provided definitive assignments of the CO stretches due to the small solubility and interference from solvent bands in this region. Conventional IR methods have not resulted in observation of the monocarbonyl species **4** in solution because it is a minority species throughout the range of conditions convenient for investigation (P_{CO} = 0.1–1 atm; T = 280–300 K).

(TTiPP)Rh•. [Tetrakis(2,4,6-triisopropylphenyl)-porphyrinato]rhodium(II) occurs as a stable metalloradical, (TTiPP)Rh• (**6**), as shown by the contact-shifted ^{1}H NMR spectrum which is closely related to that observed for (TMP)Rh•. Compound **6** failed to give an observable EPR spectrum in toluene glass (90 K), but addition of ^{13}CO to a toluene solution of **6** yields an isotropic EPR spectrum ($\langle g \rangle$ = 2.10, $\langle A(^{13}C) \rangle$ = 320 MHz) for the ^{13}CO derivative of (TTiPP)RhCO (**7**) (eq 3). Frozen

$$(TTiPP)Rh^{\bullet} + CO \rightleftharpoons (TTiPP)RhCO \quad (3)$$

toluene solutions (90 K) of the ^{13}CO derivative of **7** display three distinct g values and ^{13}C coupling constants associated with a nonlinear RhCO unit (g_1 = 2.167; g_2 = 2.138; g_3 = 2.000; $A(^{13}C_{(g_1)})$ = 318 MHz; $A(^{13}C_{(g_2)})$ = 347 MHz; $A(^{13}C_{(g_3)})$ = 305 MHz; $A(^{103}Rh_{(g_3)})$ = 65 MHz) (Figure 2). In contrast with (TMP)RhCO, lowering the temperature results in a regular increase in the intensity of the isotropic EPR of **7** which indicates

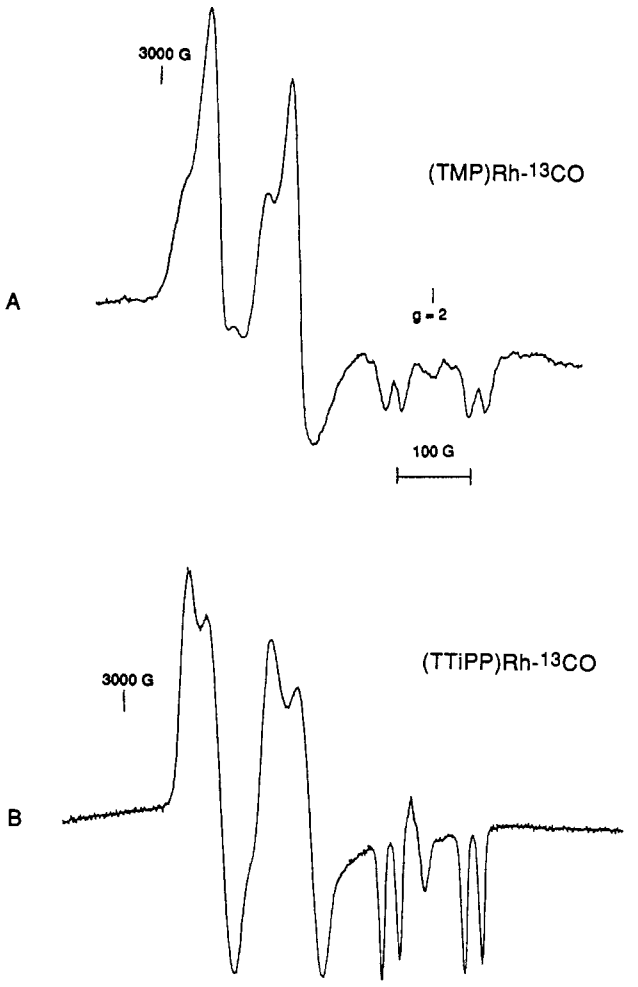

Figure 2. Frozen solution EPR spectra for (TMP)Rh^{13}CO and (TTiPP)Rh^{13}CO: (A) (TMP)Rh^{13}CO in methylcyclohexane glass (90 K) (g_1 = 2.176; g_2 = 2.147; g_3 = 1.998; $A(^{13}C_{(g_1)})$ = 313 MHz; $A(^{13}C_{(g_2)})$ = 325 MHz; $A(^{13}C_{(g_3)})$ = 302 MHz; $A(^{103}Rh_{(g_3)})$ = 65 MHz); (B) (TTiPP)Rh^{13}CO in toluene glass (90 K) (g_1 = 2.167; g_2 = 2.138; g_3 = 2.000; $A(^{13}C_{(g_1)})$ = 318 MHz; $A(^{13}C_{(g_2)})$ = 347 MHz; $A(^{13}C_{(g_3)})$ = 305 MHz; $A(^{103}Rh_{(g_3)})$ = 65 MHz).

that (TTiPP)RhCO is stable with respect to dimerization. Low-temperature ^{1}H and ^{13}C NMR in toluene also failed to yield evidence for the dimerization of **7**.

Thermodynamic and Activation Parameters for Dimerization of (TMP)RhCO. Isotropic ESR spectral intensities for (TMP)RhCO (**4**) were studied as a function of CO pressure and temperature. Solutions of (TMP)Rh• (**3**) ((0.8–2.0) × 10^{-3} M) with CO ($P_{CO} \approx$ 0.1–1.0 atm) show an increase in the EPR intensity of **4** (T = 290 K) as the P_{CO} increases up to 0.3 atm and then remains constant as P_{CO} is further increased.[8] This CO pressure dependence is associated with formation of **4** and (TMP)RhC(O)C(O)Rh(TMP) (**5**) from **3** and CO where effectively all of the (TMP)Rh• is consumed at $P_{CO} > 0.3$ atm. When the temperature of these solutions is lowered (T = 290–200 K), the intensity of the EPR spectrum of **4** regularly decreases and becomes undetectable below 220 K. This behavior is associated with an equilibrium between **4** and the C–C-bonded dimer (**5**). Analysis of the temperature dependence for the isotropic EPR intensity provides a value for the enthalpy of dimerization of **4** (ΔH°_2 = −18.3 ± 0.8 kcal mol^{-1}) (Figure 3).

The ^{1}H NMR spectrum for (TMP)RhC(O)C(O)Rh(TMP) (**5**) in toluene broadens as the temperature is elevated (230–300 K). This line broadening is ascribed to exchange of the diamagnetic dimer, **5**, with the paramagnetic monomer, **4**. The contribution of the exchange reaction to the line width at half-height is given by the general expression $T_{2(ex)}^{-1} = \pi\tau_d^{-1}[(A\tau_p/2)^2][1 + (A\tau_p/2)]^{-1}$, where $T_{2(ex)}^{-1} = T_2^{-1}(obs) - T_2^{-1}(nat)$, τ_d and τ_p are the

Table I. Guideline Bond Energy Criteria for Reactions of M–M and M• with CO That Produce Dimetal Ketones and Dimetal α-Diketones[11,12]

	$\sim\Delta H°$,[a] kcal mol^{-1}	$\sim\Delta G°$(289 K),[a,b] kcal mol^{-1}
MM + CO ⇌ MC(O)M	(MM) − 2(MC(O)) + 70	(MM) − 2(MC(O)) + 78
2M• + CO ⇌ MC(O)M	−2(MC(O)) + 70	−2(MC(O)) + 86
MM + 2CO ⇌ MC(O)C(O)M	(MM) − 2(MC(O)) + 70	(MM) − 2(MC(O)) + 86
2M• + 2CO ⇌ MC(O)C(O)M	(2(MC(O)) + 70	(2(MC(O)) + 94
MC(O)M + CO ⇌ MC(O)C(O)M	0	+8

[a] Estimated using (C≡O) − (C═O) = 70 kcal mol^{-1} and (O)CC(O) = 70 kcal mol^{-1}. [b] Estimated assuming $\Delta S°$ = 25 cal K^{-1} mol^{-1}.

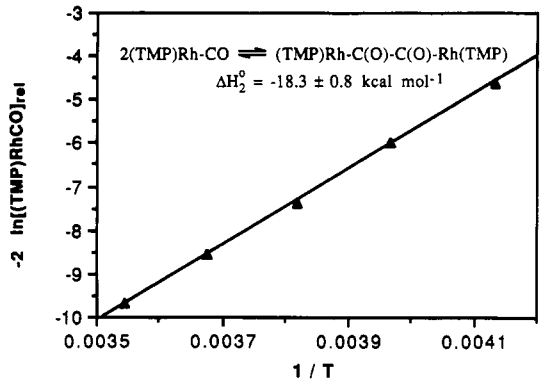

Figure 3. Van't Hoff plot for the dimerization of (TMP)RhCO using the relative EPR spectral intensity of (TMP)RhCO as the observable.

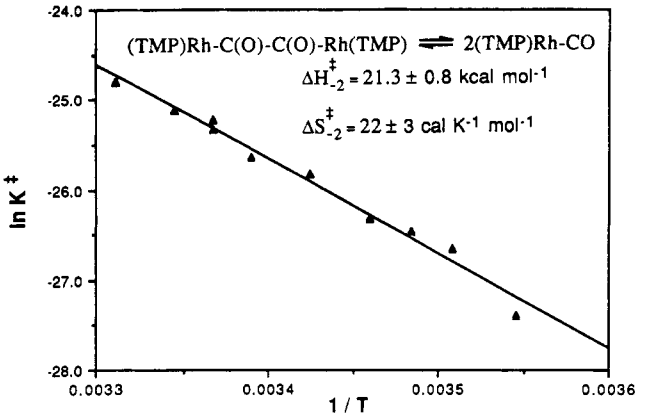

Figure 4. Determination of the activation parameters for the dissociation of **5** into **4** using ^{1}H NMR line broadening of **5** as the observable.

lifetimes of the nuclei in the diamagnetic and paramagnetic states, respectively, and A is the electron–nuclear coupling constant for the nucleus being observed.[9,10] The activation parameters for the dissociation process ($\Delta H^{\ddagger}_{-2}$ = 21.3 ± 0.8 kcal mol^{-1}; $\Delta S^{\ddagger}_{-2}$ = 22 ± 3 cal K^{-1} mol^{-1}) are obtained from the temperature dependence of the line broadening (Figure 4).

Attempts To Observe 19-Electron Metallocarbonyl Species. Diffusion of CO into frozen toluene solutions (90 K) of (TMP)Rh• results in slow and complete conversion to the five-coordinate 17-electron complex, (TMP)RhCO, with no evidence for a six-coordinate 19-electron dicarbonyl complex. Addition of THF, triethylamine, or pyridine to solutions of the (TMP)RhCO or addition of CO to frozen toluene solutions of THF and N(Et)$_3$ adducts of **3** failed to produce any evidence for six-coordinate 19-electron complexes.

Reaction of (TMP)RhCO with Hydrogen Atom Sources. Solutions that contain (TMP)RhH and (TMP)Rh• when pressurized with CO (P_{CO} ~ 0.5 atm) produce a system containing (TMP)RhH, (TMP)RhCO, and (TMP)RhC(O)C(O)Rh(TMP), but no formyl complex, (TMP)RhCHO, is detected over a period of weeks.

Benzene solutions containing an equilibrium distribution of (TMP)RhCO and (TMP)RhC(O)C(O)Rh(TMP) ([(TMP)Rh•]$_i$ ~ 1 × 10^{-3} M, P_{CO} ~ 0.6 atm) react with both (Bu)$_3$SnH and H_2 to produce the formyl complex, (TMP)RhCHO. These reactions are ascribed to 1-electron carbonyl carbon reactions of (TMP)RhCO (eqs 4 and 5).

$$\text{(TMP)RhCO} + \text{HSn(Bu)}_3 \rightarrow \text{(TMP)RhCHO} + \tfrac{1}{2}[(\text{Bu})_3\text{Sn}]_2 \quad (4)$$

$$2\text{(TMP)RhCO} + H_2 \rightleftharpoons 2\text{(TMP)RhCHO} \quad (5)$$

Reaction of (TMP)RhCO with Styrene. Benzene solutions containing preformed **4** and **5** when mixed with styrene and repressurized with CO (P_{CO} > 0.3 atm) react to form (TMP)RhC(O)CH$_2$CH(C$_6$H$_5$)C(O)Rh(TMP) (**8**) (eq 6), which is ob-

$$2\text{(TMP)RhCO} + \text{CH}_2{=}\text{CH(C}_6\text{H}_5) \rightleftharpoons \text{(TMP)RhC(O)CH}_2\text{CH(C}_6\text{H}_5\text{)C(O)Rh(TMP)} \quad (6)$$

served in solution by ^{1}H and ^{13}C NMR for the ^{13}CO derivatives. Two carbonyl carbon peaks in the ^{13}C NMR for the ^{13}CO derivative of **8** ((C$_6$D$_6$) δ = 196.58, 193.40) with one-bond ^{103}Rh–^{13}C coupling (31, 36 Hz) and two-bond ^{13}C–H couplings ($^2J_{^{13}C-H}$ = 4.6–6.5 Hz) is particularly diagnostic for **8**. No evidence was found for alkyl-bridged complexes which form from the reaction of (TMP)Rh• with alkenes.

Discussion

Porphyrin Ligand Steric Effects on the Reactions of Rhodium(II) Porphyrins with CO. Rhodium(II) porphyrins are unusual in fulfilling the thermodynamic requirements to chemically reduce CO in forming dimetal ketone, MC(O)M, and dimetal α-diketone, MC(O)C(O)M, complexes.[3,11,12] Formation of a dimetal α-diketone in equilibrium with a dimetal ketone has particularly demanding thermodynamic criteria, because in addition to the need for relatively large absolute M–C bond energies, the effective M–C bond energy in the α-diketone must exceed that in the metalloketone by a minimum of 4–5 kcal mol^{-1} (Table I).[3,11] This latter criterion is attainable by rhodium(II) porphyrin complexes because the bent single-atom-bridged metalloketone species are more sensitive to the steric demands of the porphyrin ligands than the two-atom-bridged MC(O)C(O)M complexes where the two porphyrin rings are further apart and capable of attaining a nearly parallel orientation. Structure simulations given below for (OEP)RhC(O)Rh(OEP) and (OEP)RhC(O)C(O)Rh(OEP) illustrate the steric congestion in the dimetal ketone that is relieved in the dimetal diketone.

Steric effects in the metalloketone species are manifested in the equilibrium distribution of complexes observed for a series of rhodium porphyrin derivatives that have increasing steric demands (OEP < TXP < TMP < TTiPP). In the (OEP)Rh system the metalloketone is the major species at all conditions studied (P_{CO} = 0.1–30 atm; T = 220–300 K), in the (TXP)Rh system it is a minor species observed only at low pressure (P_{CO} < 0.4 atm; T = 298 K), and metalloketone species are not observed at any conditions in reactions of CO with (TMP)Rh• and (TTiPP)Rh•. Decline in the thermodynamic stability of the metalloketone in the (TXP)Rh and (TMP)Rh systems results in dramatic increases

(9) (a) McConnel, H. M.; Berger, S. B. *J. Chem. Phys.* **1957**, *27*, 230. (b) Kreilich, R. W.; Weissman, S. I. *J. Am. Chem. Soc.* **1966**, *88*, 2645. (c) Johnson, C. S., Jr. *Advances in Magnetic Resonance*; Academic: New York, 1965; Vol. I, p 33.

(10) Williams, D. J.; Kreilick, R. *J. Am. Chem. Soc.* **1967**, *89*, 3408. Williams, D. J.; Kreilick, R. *J. Am. Chem. Soc.* **1968**, *90*, 2775.

(11) Wayland, B. B.; Coffin, V. L.; Sherry, A. E.; Brennen, W. R. *ACS Symp. Ser.* **1990**, *428*, 148–158.

(12) Wayland, B. B. *Polyhedron* **1988**, *7*, 1545.

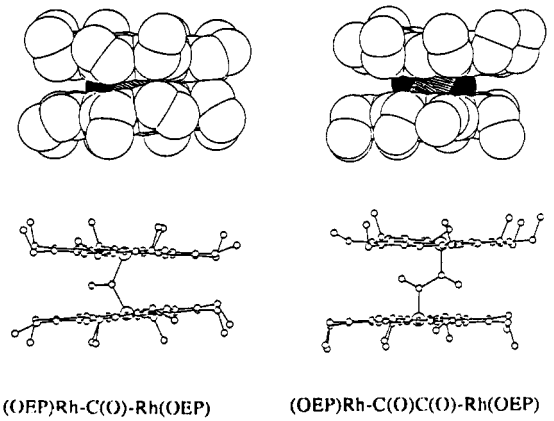

(OEP)Rh-C(O)-Rh(OEP) (OEP)Rh-C(O)C(O)-Rh(OEP)

in the α-diketone species where at P_{CO} = 1 atm and T = 298 K greater than 99% of the rhodium porphyrin is incorporated into a CO reductive coupling product, RhC(O)C(O)Rh. Further increase in the ligand steric demands associated with the (TTiPP)Rh• complex inhibits the CO coupling reaction. Similarly, the monocarbonyl complex, (RhCO)•, is unobserved for (OEP)Rh and (TXP)Rh, a minor species with (TMP)Rh• and the major species for the (TTiPP)Rh• system.

1-Electron Activation of CO. Activation of CO by 1-electron steps is best known for radicals of the representative elements like methyl radicals which react with CO to form the transient acetyl radical ($CH_3\dot{C}O$).[13] The acetyl radical is an example of 1-electron-activated CO because it subsequently reacts by a second 1-electron reaction at the carbonyl carbon to produce acetone, $(CH_3)_2CO$, and biacetyl, $CH_3C(O)C(O)CH_3$ (eqs 7–9).

$$CH_3^\bullet + CO \rightarrow CH_3\dot{C}O \quad (7)$$

$$CH_3\dot{C}O + CH_3^\bullet \rightarrow (CH_3)_2CO \quad (8)$$

$$2CH_3\dot{C}O \rightarrow CH_3C(O)C(O)CH_3 \quad (9)$$

In transition-metal chemistry 1-electron activation of CO has been accomplished by reduction of 18-electron metal carbonyl complexes to form transient 19-electron species like $[(CO)_4FeCO]^{\bullet-}$.[14,15] One important reaction of 19-electron carbonyl complexes is hydrogen atom abstraction from metal hydrides to form transient 18-electron metalloformyl species (eq 10).[15] Comparable reactivity has also been observed for $[(CO)_5CrCO]^{\bullet-}$[16] and other 19-electron metallocarbonyl complexes.[17]

$$[(CO)_4FeCO]^{\bullet-} + HM \rightarrow (CO)_4FeC(O)H + [M^\bullet] \quad (10)$$

(Octaethylporphyrin)rhodium(II) dimer, $[(OEP)Rh]_2$, reacts with CO to produce equilibrium distributions of dimetal ketone, (OEP)RhC(O)Rh(OEP), and dimetal α-diketone, (OEP)RhC(O)C(O)Rh(OEP), complexes.[2,3] These products have a formal relationship to acetone, $CH_3C(O)CH_3$, and biacetyl, $CH_3C(O)C(O)CH_3$, that result from the reactions of $CH_3^\bullet$ with CO which suggested that (OEP)RhCO may function like an acyl radical intermediate. Kinetic studies have also implicated a monocarbonyl intermediate in the $[(OEP)Rh]_2$-catalyzed reaction of (OEP)RhH with CO that produces the metalloformyl complex, (OEP)RhCHO.[18] Initial efforts to observe the proposed intermediate complex, (OEP)RhCO, directly by EPR were not successful, because of the vanishingly small concentrations of these species. Reactions of the more sterically demanding (TMP)Rh• and (TTiPP)Rh• with CO have resulted in sufficient equilibrium concentrations of the 17-electron monocarbonyl species, (TMP)RhCO and (TTiPP)RhCO, to permit direct observation by EPR and evaluation of the reactivity patterns for these species.

(TMP)RhCO and (TTiPP)RhCO. The large steric requirements of tetramesitylporphyrin (TMP) and tetrakis(2,4,6-triisopropylphenyl)porphyrin (TTiPP) preclude dimerization through M–M bonding and provide stable monomeric Rh^{II} complexes, (TMP)Rh• (**3**) and (TTiPP)Rh• (**6**). Compounds **3** and **6** have closely related contact shifted ^1H NMR spectra that conform with Curie–Weiss behavior. EPR spectra for **3** in toluene glass (90 K) ($g_\perp$ = 2.65; $g_\parallel$ = 1.915) clearly indicate that this low-spin d^7 ($S = {}^1/_2$) complex has a $(d_{xz}d_{yz}d_{xy})^6d_{z^2}{}^1$ electron configuration.

(TMP)Rh• (**3**) reacts with CO to produce an equilibrium distribution of **3** with (TMP)RhCO (**4**) and a C–C-bonded dimer, (TMP)RhC(O)C(O)Rh(TMP) (**5**) (eqs 1 and 2). At pressures of CO greater than 0.3 atm ($T \leq$ 298 K) virtually all of the porphyrin is converted to an equilibrium distribution of **4** and **5** where **4** is the minor species (<1%). Reaction of CO ($P_{CO} \sim$ 0.1–1.0 atm; T = 220–300 K) with (TTiPP)Rh• (**6**) produces an equilibrium of **6** with (TTiPP)RhCO (**7**) as observed by EPR and a ^1H NMR associated with the fast exchange of **6** with **7**. ^1H NMR down to 283 K fails to reveal observable quantities of a C–C-bonded dimer of (TTiPP)RhCO. Inter-porphyrin repulsions between TTiPP ligands apparently prohibit sufficiently close approach of (TTiPP)RhCO units to permit CO coupling. A dimetal ketone, MC(O)M, which is the major species in the reaction of $[(OEP)Rh]_2$ with CO is not observed in either the (TMP)Rh or (TTiPP)Rh systems due to the inability of the bent one-atom-bridged species to accommodate the steric demands of these ligands.

The EPR g values for **4** (g_1 = 2.176; g_2 = 2.147; g_3 = 1.998) and **7** (g_1 = 2.167; g_2 = 2.138; g_3 = 2.000) are consistent with the unpaired electron occupying a molecular orbital that is an admixture of rhodium d_{z^2} with CO σ (2s, 2p) character. Deviations of the g values from the free-electron value are dominated by intermixing of the d_{xz} and d_{yz} with d_{z^2} by spin–orbit coupling. Observation of three g values indicates that the d_{xz} and d_{yz} are nondegenerate, which means that these complexes do not have a 3-fold or higher axis of symmetry. The removal of degeneracy of the d_{xz} and d_{yz} is ascribed to the presence of a nonlinear RhCO unit which is anticipated for the 7-electron case ($d^7 + \pi^{*0}$) when the metal and diatomic molecule are capable of relatively strong covalent σ bonding. A linear MCO unit maximizes the dπ–pπ bonding while bending the MCO unit splits the CO π* degeneracy, yielding one orbital that retains the π* character and one orbital appropriate for σ bonding with d_{z^2}.[19] Bending of the MCO unit will occur only when the improvement in σ covalent bonding is more important than the decline in the dπ–pπ bonding. (por)RhCO complexes are electronically related to the more familiar (por)FeNO complexes[19–22] in that the sum of the nd and the π* electrons is 7 [(Rh^{II}, d^7; CO, π^{*0})(Fe^{II}, d^6; NO, π^{*1})] and both the $Rh^{II}CO$ and $Fe^{II}NO$ species have nonlinear metal diatomic units. The bent MCO units observed in **4** and **7** are precedented

(13) (a) Watkins, K. W.; Word, W. W. *Int. J. Chem. Kinet.* **1974**, *6*, 855–873. (b) Anastasi, C.; Maw, P. L. *J. Chem. Soc., Faraday Trans. 1* **1982**, *78*, 2423. (c) O'Neal, H. E.; Benson, S. W. *Thermochemistry of Free Radicals*; Kochi, J. K., Ed.; Wiley: New York, 1973; Vol. 2, Chapter 17.

(14) Fairhurst, S. A.; Morton, J. R.; Preston, K. F. *J. Chem. Phys.* **1982**, *77*, 5872.

(15) (a) Amatore, C.; Verpeaux, J. N.; Krusic, P. J. *Organometallics* **1988**, *7*, 2426. (b) Narayanan, B. A.; Amatore, C.; Kochi, J. K. *Organometallics* **1986**, *5*, 926.

(16) Narayanan, B. A.; Kochi, J. K. *J. Organomet. Chem.* **1984**, *272*, C49.

(17) Symons, M. C. R.; Bratt, S. W. *J. Chem. Soc., Dalton Trans.* **1979**, 1739.

(18) Paonessa, R. S.; Thomas, N. C.; Halpern, J. *J. Am. Chem. Soc.* **1985**, *107*, 4333.

(19) (a) Wayland, B. B.; Minkiewicz, J. V.; Abd-Elmageed, M. E. *J. Am. Chem. Soc.* **1974**, *96*, 2795. (b) Hoffman, R.; Chen, M. M. L.; Thorn, D. L. *Inorg. Chem.* **1977**, *16*, 503. (c) Enemark, J. H.; Feltham, R. D. *Coord. Chem. Rev.* **1974**, *13*, 339.

(20) (a) Wayland, B. B.; Olson, L. W. *J. Am. Chem. Soc.* **1974**, *86*, 6037. (b) Kon, H.; Kataoka, N. *Biochemistry* **1969**, *8*, 4757. (c) Oosterhuis, W. T.; Lang, G. *J. Chem. Phys.* **1969**, *50*, 4381. (d) Morse, R. H.; Chan, S. I. *J. Biol. Chem.* **1980**, *255*, 7876.

(21) (a) Piciulo, P. L.; Rupperecht, G.; Scheidt, W. R. *J. Am. Chem. Soc.* **1974**, *96*, 5293. (b) Scheidt, W. R.; Piciulo, P. L. *J. Am. Chem. Soc.* **1976**, *98*, 1913. (c) Scheidt, W. R.; Frisse, M. E. *J. Am. Chem. Soc.* **1975**, *97*, 17. (d) Scheidt, W. R.; Brinegar, A. C.; Ferro, E. B.; Kirner, J. F. *J. Am. Chem. Soc.* **1977**, *99*, 7315.

(22) (a) Hori, H.; Ikeda-Saito, M.; Yonetani, T. *J. Biol. Chem.* **1981**, *256*, 7849. (b) Kon, H. *J. Biol. Chem.* **1968**, *243*, 4350. (c) Chien, J. C. W. *J. Chem. Phys.* **1969**, *51*, 4220. (d) Dickinson, L. C.; Chien, J. C. W. *J. Am. Chem. Soc.* **1971**, *93*, 5036. (e) Dickinson, L. C.; Chien, J. C. W. *Biochem. Biophys. Res. Commun.* **1974**, *59*, 1292. (f) Henry, Y.; Banerjee, R. *J. Mol. Biol.* **1973**, *73*, 469. (g) Doetschman, D. C.; Utterback, S. G. *J. Am. Chem. Soc.* **1981**, *103*, 2847.

only by 19-electron complexes like $[Fe(CO)_5]^{\bullet-}$[14] where the odd electron is required to occupy a predominantly ligand (CO) based orbital. (por)RhCO complexes are at present the only examples where a bent MCO unit is induced by effective M–CO σ bonding.

Isotropic ^{13}C coupling constants of 313 and 320 MHz, respectively, for **4** and **7** correspond to a C_{2s} density of 0.10 ($\rho_{C_{2s}} = \langle A(^{13}C)\rangle/3110$ MHz), which is intermediate between the C_{2s} spin densities for $[(Fe(CO)_5]^{\bullet-}$ (0.07)[14] and [HĊO] (0.12).[23] The observed variation of the ^{13}C hyperfine coupling constant along the three principal directions of the **g** tensor is associated with the C_{2p} spin density. Determination of the C_{2p} spin density ($\rho_{C_{2p}} = B(^{13}C)/90.8$ MHz) requires the principal values for the $A(^{13}C)$ tensor but the probable noncoincidence of the principal directions for the **g** and $A(^{13}C)$ tensors precludes an accurate evaluation of these values from the glass EPR spectrum for a low-symmetry complex (C_s or C_1). However, the lower limit for the C_{2p} spin density can be obtained because the maximum anisotropy ($A(^{13}C(\max)) - \langle A\rangle$) cannot exceed $2B$. This restriction places lower limits of 0.08 and 0.15 for the C_{2p} spin densities for **4** and **7**, respectively, and thus lower limits on the CO spin densities of 0.18 and 0.25. The odd electron thus has substantial CO character but is primarily located on the rhodium porphyrin unit.

The electronic structures of **4** and **7** are between the limiting electron structures that localize the odd electron either in the rhodium d_{z^2} (•Rh:C≡O) or on the carbonyl carbon (Rh—Ċ=O). The 17-electron carbonyl complex, (TMP)RhCO, is thus poised for a second 1-electron reaction at either the rhodium or carbonyl carbon sites. Reaction of **4** with a 1-electron species X• at the metal produces an 18-electron Rh(III) carbon monoxide complex, (TMP)Rh(X)(CO), while reaction at the carbonyl carbon forms a 16-electron Rh(III) complex, (TMP)RhC(O)X. All of the 1-electron radical-like reactions of (TMP)RhCO that have been observed occur at the carbonyl carbon to form 16-electron rhodium(III) complexes. To our knowledge, this reactivity pattern of **4** is currently unique among 17-electron metal carbonyls.

Dimerization of (TMP)RhCO by C–C Bond Formation. Reversible dimerization of (TMP)RhCO (**4**) through C–C bond formation to produce a 1,2-ethanedionyl complex, (TMP)RhC(O)C(O)Rh(TMP) (**5**) (eq 2), illustrates a carbonyl carbon centered 1-electron reaction that can be viewed as an organometallic analog of formyl radical coupling (2HĊO → HC(O)C(O)H).

Rhodium(II) porphyrins are currently the only metal complexes known to form α-diketone complexes, MC(O)C(O)M, from reaction with CO. The only other reported α-diketone complexes were prepared as kinetic products from reactions of metal pentacarbonyl anions $[M(CO)_5]^-$ (M = Mn, Re) with oxalyl chloride, ClC(O)C(O)Cl.[24] X-ray structural characterization of $(CO)_5ReC(O)C(O)Re(CO)_5$ shows the presence of a trans-planar ReC(O)C(O)Re unit. (TXP)RhC(O)C(O)Rh(TXP) and the TMP derivative have two CO stretching frequencies, which is indicative of a nonplanar α-diketone unit. Structure simulations illustrate that the trans-planar structure has unfavorable interactions between the carbonyl oxygens and the porphyrin ring, which are substantially relieved through rotation by 20–30° around the (O)C–C(O) bond axis. Observation of two CO stretching frequencies and nonplanar dionyl units in diaryl α-diketones are similarly ascribed to unfavorable interactions of the carbonyl oxygen with the phenyl ring attached to the adjacent carbonyl carbon.[25]

Temperature dependence of the isotropic EPR intensity for (TMP)RhCO (**4**) has been analyzed to provide the enthalpy change for reaction 2 ($\Delta H^\circ_2 = -18.3 \pm 0.8$ kcal mol^{-1}) (Figure 3). Temperature dependence of the pyrrole ^1H NMR line broadening of (TMP)RhC(O)C(O)Rh(TMP) (**5**) is ascribed to exchange of the diamagnetic dimer (**5**) with the paramagnetic monomer (**4**) and used in deriving the activation energy for dissociation ($\Delta H^\ddagger_{-2} = 21.3 \pm 0.8$ kcal mol^{-1}) (Figure 4). An energy profile for the reversible dimerization of (TMP)RhCO is illustrated in Figure 5. The activation enthalpy for dimerization ($\Delta H^\ddagger_2 \sim 3$ kcal mol^{-1}) is derived from ΔH°_2 (−18.3 ± 0.8 kcal mol^{-1}) and $\Delta H^\ddagger_{-2}$ (21.3 ± 0.8 kcal mol^{-1}) and found to be close to the value calculated for a diffusion-controlled process in benzene (3.1 kcal).[26] Assuming that the dionyl unit, –C(O)C(O)–, in **5** is similar to that in organic analogues like biformyl, the dissociation of **5** into **4** results in cleavage of a 65–70-kcal C–C bond.[11,12] Carbon–carbon bond homolysis without structural and electronic reorganization of the resulting (TMP)RhĊ=O unit would have an enthalpy change ($\Delta H^\circ \sim 65$–70 kcal mol^{-1}) which is substantially larger than the observed dissociation energy of **5** ($\Delta H^\circ_{-2} = 18.3 \pm 0.8$ kcal mol^{-1}). This result means that (TMP)RhCO is approximately 25 kcal mol^{-1} lower in energy than the hypothetical localized carbon-based radical, (TMP)RhĊ=O, and this result further implies that (TMP)RhCO contains only a partially rehybridized carbonyl unit with a bond order between 2 and 3 (Rh—C⋯O). The current maximum observed Rh–C(O)X bond energy of ~58 kcal mol^{-1} [3,12] is insufficient to justify full rehybridization of C≡O to a C=O unit which occurs with the expense of ~70 kcal mol^{-1}. More complete CO rehybridization occurs in the formyl radical because of the stronger H–C(O) bond. In the case of (por)RhCO complexes, complete reduction of the C–O bond order to 2 requires formation of a second bond at the carbonyl carbon.

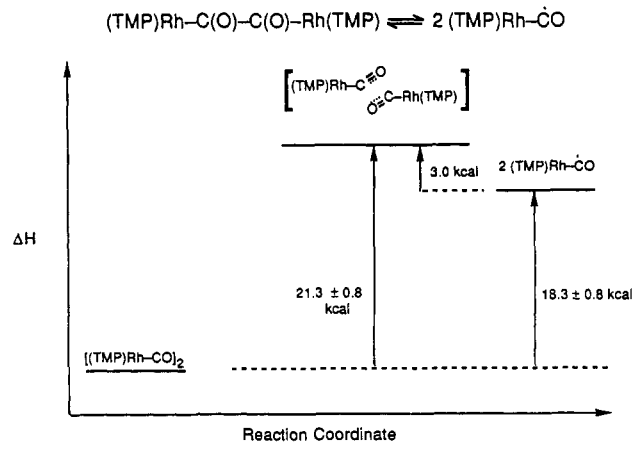

Figure 5. Enthalpy profile for the dissociation of **5** into **4**.

Thermodynamic and kinetic parameters for the dissociation of (TMP)RhC(O)C(O)Rh(TMP) provide a detailed view of how the nature of (TMP)RhCO provides a facile pathway for (O)C–C(O) bond homolysis. The stretching and ultimate cleavage of the C–C bond is synchronized with an increase in the CO bond order such that the activation enthalpy for dissociation ($\Delta H^\ddagger_{-2} = 21.3 \pm 0.8$ kcal mol^{-1}) is substantially smaller than the C–C bond energy of ~65–70 kcal mol^{-1} expected for α-diketone species.[27-29] The RhCO units in the transition state are thus similar to the monomer, (TMP)RhCO. Most of the energy expended for rehybridization of the carbonyl unit in forming the C–C bond in **5** (reaction 2) is regained in the transition state for the dissociation of **5** where an increase in the C–O bond order occurs at the expense of weakening the C–C bond. Similarly, homolytic dissociation energies and potentially associated activation energies for dissociation of any X• from (por)RhC(O)X should be ~20–25 kcal mol^{-1} less than the C(O)X bond energy.

(23) (a) Holmberg, R. W. *J. Chem. Phys.* **1969**, *51*, 3255. (b) Cochran, E. L.; Adrian, F. J.; Bowers, V. A. *J. Chem. Phys.* **1966**, *44*, 4626.
(24) de Boer, E. J. M.; de With, J.; Meijboom, N.; Orpen, A. G. *Organometallics* **1985**, *4*, 259.
(25) (a) Juarez, M.; Martin-Lomas, M.; Ballanato, J. *An. Quim.* **1976**, *72*, 607. (b) Bellanato, J.; Juarez, H.; Martin-Lomas, M. *Ibid.* **1978**, *74*, 1355.
(26) Estimated from the temperature dependence of the viscosity (η) of C_6D_6 using the expression $k_{diff} = 8RT/30\eta$. Calvert, J. G.; Pitts, J. N., Jr. *Photochemistry*; Wiley: New York, 1966; p 626.
(27) Wagman, D. D.; Evans, W. H.; Parker, V. B.; Halow, I.; Bailey, S. M.; Schumm, R. H. *NBS Technical Note 270-3*; Institute for Basic Standards, National Bureau of Standards: Washington, DC, 1968.
(28) Cox, J. D.; Pilcher, G. *Thermochemistry of Organic and Organometallic Compounds*; Academic: New York, 1970.
(29) Benson, S. W. *Thermochemical Kinetics*; Wiley: New York, 1968.

This feature of (por)RhC(O)X species can be contrasted with organic analogues, $CH_3C(O)X$, where the X–C(O) bond homolysis enthalpies approach the values for the X–C(O) bond energies.[29]

19-Electron complexes like $[Cr(CO)_6]^{\bullet-}$ which are essentially forced to react at the carbonyl carbon should rapidly dimerize by radical coupling to form $[(CO)_5CrC(O)C(O)Cr(CO)_5]^{2-}$. The radical coupling process, $2MCO \rightarrow MC(O)C(O)M$, can be expected to have favorable thermodynamics, but the resulting dionyl complex is most probably a transient that is unstable relative to loss of CO. The isoelectronic complex $(CO)_5ReC(O)C(O)Re(CO)_5$ has sufficient kinetic stability to be studied in solution, but it is thermodynamically unstable relative to loss of CO with formation of $Re_2(CO)_{10}$ even at high CO pressures ($P_{CO} \sim 100$ atm).[24] (TMP)RhC(O)C(O)Rh(TMP) (**5**) is different from the dionyl complex of $Re(CO)_5$ in that **5** is kinetically unstable in the sense that the C–C bond rapidly dissociates and re-forms but is thermodynamically the dominant species at equilibrium ($P_{CO} >$ 0.3 atm; T = 298 K). The greater kinetic stability toward (O)C–C(O) bond cleavage for $(CO)_5ReC(O)C(O)Re(CO)_5$ compared to **5** probably results from the presence of electronically saturated (18-electron) metal centers. The 18-electron rhenium center is ineffective in assisting the reorganization of $(CO)_5Re\dot{C}{=}O$ because it would produce a 19-electron metal center. This contrasts with **5** where formation of a 17-electron rhodium center can be effective in the reorganization of the hypothetical carbon-based radical, (TMP)Rh$\dot{C}$=O.

Reactions of (TMP)RhCO with Hydrogen Atom Sources. (TMP)RhCO fails to react at a finite rate with (TMP)RhH to produce a formyl complex. This behavior is in contrast with the (OEP)Rh system where the reaction of (OEP)RhH with a proposed monocarbonyl intermediate, (OEP)RhCO, is implicated in producing the formyl complex, (OEP)RhCHO.[18] Steric requirements of the TMP ligand must prohibit achieving the transition state necessary for H atom transfer to the carbonyl center. The trajectory for H atom transfer probably requires a Rh–C(O)–H angle of ~120°, and this structure would place the two TMP ligands in an untenable proximity. Dimerization of (TMP)RhCO through C–C bonding can occur with a nearly parallel orientation of the two porphyrin planes which minimizes interligand repulsions. Related steric effects in the transition state have been proposed to account for the ability of (TMP)Rh$^{\bullet}$ to react selectively with methane C–H bonds in benzene solvent.[30] While methane will accommodate a four-centered transition state (Rh···CH_3···H···Rh) with parallel porphyrin planes, reaction of aromatic C–H bonds requires a bent four-centered transition state which is sterically precluded for two (TMP)Rh units.

Reaction of (TMP)RhCO with $(Bu)_3SnH$ to form (TMP)RhCHO provides an illustration of a metal hydride transferring a hydrogen atom to the carbonyl carbon. This type of reactivity should occur for a broad class of metal hydride species where steric constraints for the approach of the MH to (TMP)RhCO are not too demanding.

Benzene solutions of (TMP)Rh$^{\bullet}$ (**3**) (1×10^{-3} M) react with CO and H_2 (P_{CO} = 0.50 atm; P_{H_2} = 0.25 atm) to produce (TMP)RhCHO as the exclusive observed product. The known reaction of (TMP)Rh$^{\bullet}$ with H_2 to form (TMP)RhH is essentially eliminated in the presence of CO ($P_{CO} > 0.3$ atm) because the reaction of **3** with CO is fast and virtually all of **3** is converted to an equilibrium distribution of **4** and **5**. Independent studies have shown that (TMP)RhH fails to react with either CO or (TMP)RhCO at a finite rate, and thus the formyl complex must form by a different pathway. One possible route involves reaction of H_2 with two (TMP)RhCO units through a four-centered transition state. This proposed mechanism is related to the pathway utilized in reactions of metalloradicals with H_2 (M$^{\bullet}$···H··H···$^{\bullet}$M)[31] and recently suggested for the reaction of (TMP)Rh$^{\bullet}$ with methane (M$^{\bullet}$···H_3C···H···$^{\bullet}$M).[30]

Reaction of Styrene with (TMP)RhCO. Alkenes are known to react rapidly with rhodium(II) porphyrins by radical-like processes to form alkyl-bridged complexes (por)Rh$CH_2CH(X)$-Rh(por). The reaction of styrene with (TMP)RhCO provides another opportunity to examine whether the Rh(II) metal based radical ($^{\bullet}$Rh:C≡O:) or acyl radical (Rh—$\dot{C}$=O) nature is manifested. When the equilibrium distribution of (TMP)RhC-(O)C(O)Rh(TMP) and (TMP)RhCO is preformed at CO pressures where virtually all of the (TMP)Rh$^{\bullet}$ is reacted (P_{CO} > 0.3 atm), subsequent reaction with styrene forms (TMP)-$RhC(O)CH_2CH(C_6H_5)C(O)Rh(TMP)$ as the only observed species in the ^1H NMR. Presumably, (TMP)RhCO interacts with styrene to form an intermediate of the form (TMP)RhC(O)-$CH_2\dot{C}H(C_6H_5)$ which is trapped by a second (TMP)RhCO. The styrene reaction is further evidence that (TMP)RhCO has a strong preference to function like an acyl rather than a metal-based radical.

Comparison of (TMP)RhCO with Related 17-Electron d^7 Metal Carbonyl Complexes. An extensive series of 17-electron d^7 pentacarbonyl complexes ($M(CO)_5$: M = Fe^+, Os^+, Mn^0, Re^0, Cr^-, Mo^-, W^-) have been investigated as transient species or in dilute crystals and low-temperature matrices.[32-35] Spectroscopic studies for each of these five-coordinate d^7 complexes have been consistent with C_{4v} symmetry associated with a square-pyramidal array of CO ligands, and EPR studies place the unpaired electron in an orbital of a_1 symmetry (d_{z^2} + CO σ) that is directed at the apical CO.[32,35] The general features of the electronic and geometric structures of these pentacarbonyl complexes are thus related to (TMP)RhCO, but none of these complexes have yet been reported to have either a significantly bent MCO unit or carbon-centered 1-electron reactions. 17-Electron pentacarbonyl complexes do manifest reactivity characteristic of radicals such as dimerization and atom abstractions, but these 1-electron reactions are reported to occur exclusively at the metal center to produce 18-electron complexes.[32] Persistent 17-electron metal carbonyls provide better candidates for structural and reactivity comparisons with (TMP)RhCO. One particularly appropriate example is the 17-electron d^7 complex *trans*-$(PCy_3)_2(CO)_2ReCO$ which has a unique CO in the apical position of an idealized square-based pyramid[36] and the odd electron in a (d_{z^2} + CO σ) molecular orbital.[37] This complex has structural and electronic features in common with (TMP)RhCO yet fails to dimerize by C–C bonding and reacts with H_2 and Bu_3SnH to form only the metal hydride, $(PCy_3)_2$-$(CO)_3ReH$. Absence of dimerization by C–C binding must be thermodynamic in origin. The steric bulk of the PCy_3 ligand which blocks dimerization by Re–Re bonding is close to the Re site and may also inhibit dimerization by CO coupling. Porphyrin ligand steric effects result from substituents on the periphery and thus provide better opportunities to selectively block M–M bonding and yet retain access to the vicinity of the metal center.

Bonding factors are also important in determining the difference in reactivity of 17-electron metal carbonyls. Reactions of (M—CO)$^{\bullet}$ that produce reduced carbonyl (C=O) units can be viewed as occurring through a metalloacyl radical (M—$\dot{C}$=O) where

(30) Sherry, A. E.; Wayland, B. B. *J. Am. Chem. Soc.* **1990**, *112*, 1259.
(31) (a) Halpern, J.; Pribanic, M. *Inorg. Chem.* **1970**, *9*, 2616. (b) Simandi, L. I.; Nagy, F. *Acta Chim. Acad. Sci. Hung.* **1965**, *46*, 101. (c) Simandi, L. I.; Budo-Zahonyi, E.; Szverenyi, Z.; Nemeth, S. *J. Chem. Soc., Dalton Trans.* **1980**, 276. (d) Halpern, J. *Inorg. Chim. Acta* **1982**, *62*, 31.
(32) Baird, M. C. *Chem. Rev.* **1988**, *88*, 1217.
(33) (a) Meckstroth, W. K.; Walters, R. T.; Waltz, W. L.; Wojcicki, A.; Dorfman, L. M. *J. Am. Chem. Soc.* **1982**, *104*, 1842. (b) Church, S. P.; Hermann, H.; Grevels, F. W.; Schaffner, K. *J. Chem. Soc., Chem. Commun.* **1984**, 785. (c) Yasufuku, K.; Noda, H.; Iwai, J.; Ohtani, H.; Hoshino, M.; Kobayashi, T. *Organometallics* **1985**, *4*, 2174. (d) Kobayashi, T.; Ohtani, H.; Noda, H.; Teratani, S.; Yasufuku, K. *Organometallics* **1986**, *5*, 110.
(34) (a) Breeze, P. A.; Burdett, J. K.; Turner, J. J. *Inorg. Chem.* **1981**, *20*, 3369. (b) Howard, J. A.; Mile, B.; Morton, J. R.; Preston, K. F.; Sutcliffe, R. *J. Phys. Chem.* **1986**, *90*, 1033.
(35) (a) Lionel, T.; Morton, J. R.; Preston, K. F. *J. Chem. Phys.* **1982**, *76*, 234. (b) Peake, B. M.; Symons, M. C. R.; Wyatt, J. L. *J. Chem. Soc., Dalton Trans.* **1983**, 1171. (c) Lionel, T.; Morton, J. R.; Preston, K. F. *J. Magn. Reson.* **1982**, *49*, 225. (d) Church, S. P.; Poliakoff, M.; Timney, J. A.; Turner, J. J. *J. Am. Chem. Soc.* **1981**, *103*, 7515. (e) Howard, J. A.; Morton, J. R.; Preston, K. F. *Chem. Phys. Lett.* **1981**, *83*, 226. (f) Symons, M. C. R.; Sweany, R. L. *Organometallics* **1982**, *1*, 834.
(36) Crocker, L. S.; Heinekey, D. M. *J. Am. Chem. Soc.* **1989**, *111*, 405.
(37) Walker, H. W.; Rattinger, G. B.; Belford, R. L.; Brown, T. L. *Organometallics* **1983**, *2*, 775.

the metal carbonyl unit is the same as in the product (eq 11). Subsequent reaction of (M—Ċ=O) with substrates will have similar thermodynamic values for all acyl radicals. Using standard organic bond energies results in enthalpy estimates for several generalized reactions of MĊ=O that have been observed for rhodium(II) porphyrins (eqs 11–14).[12] A fully rehybridized

$$M—CO^{\bullet} \rightleftharpoons M—\dot{C}=O \quad (11)$$

$$\Delta H^{\circ}_{11} = \text{negative reorganization energy}$$

$$2M—\dot{C}=O \rightleftharpoons MC(O)C(O)M \quad (12)$$

$$\Delta H^{\circ}_{12} \sim -65 \text{ to } -70 \text{ kcal mol}^{-1}$$

$$2M—\dot{C}=O + H_2 \rightarrow 2MC(O)H \quad (13)$$

$$\Delta H^{\circ}_{13} \sim -70 \text{ kcal mol}^{-1}$$

$$2M—\dot{C}=O + CH_2=CH_2 \rightarrow MC(O)CH_2CH_2C(O)M \quad (14)$$

$$\Delta H^{\circ}_{14} \sim -100 \text{ kcal mol}^{-1}$$

metalloacyl radical will have favorable thermodynamics for CO coupling and reactions with H_2 and alkenes (eqs 12–14). This approach focuses attention on the energy required to convert a 17-electron metal carbonyl $(MCO)^{\bullet}$ to the acyl radical (MĊ=O) as a source for differences in the thermodynamic capability for accomplishing reactions that produce ketone-like CO units. In the specific case of rhodium(II) porphyrins the energy to convert $(MCO)^{\bullet}$ to MĊ=O is approximately 25 kcal mol^{-1} (Table II) ($2\Delta H^{\circ}_{11} \sim 50$ kcal mol^{-1}), and thus the overall reactions that convert the monocarbonyl to ketone-like products (eqs 11–14) are thermodynamically favorable.

Any factor that stabilizes $(MCO)^{\bullet}$ relative to MĊ=O will have a detrimental thermodynamic effect on forming MC(O)X relative to other products such as XMCO. Metal–CO σ covalent bonding promotes the bending and rehybridization of the MCO unit and thus reduces ΔH°_{12}, but M–CO $d\pi$–$p\pi$ bonding, which is maximized by a linear MCO, increases ΔH°_{12}. Variation in $d\pi$–$p\pi$ bonding is thus one factor that will produce differences in the reorganization energy for transition-metal $(MCO)^{\bullet}$ complexes. The relatively low metal oxidation states and associated effective $d\pi$–$p\pi$ bonding in most 17-electron metal carbonyls undoubtedly disfavors acyl radical-like reactions of these species relative to $(por)Rh^{II}CO$ complexes.

Summary

Porphyrin ligand steric effects are used in selectively inhibiting Rh–Rh bonding and the bent one-atom-bridged dirhodium ketones, RhC(O)Rh, which results in nearly quantitative CO reductive coupling to form dirhodium α-diketones of (TXP)Rh and (TMP)Rh at mild conditions ($P_{CO} \sim 1$ atm; $T \sim 298$ K). Further increase in the ligand steric demands to TTiPP inhibits CO coupling. $(TMP)Rh^{\bullet}$ and $(TTiPP)Rh^{\bullet}$ react with CO to form 17-electron monocarbonyl species **4** and **7** that have nonlinear RhCO units and reactivity similar to that of an acyl radical. Dimerization of **4** through C–C bonding, reactions with hydrogen atom sources to produce the formyl complex, (TMP)RhCHO, and reaction with styrene to form $(TMP)RhC(O)CH_2CH(C_6H_5)C(O)Rh(TMP)$ illustrate that **4** contains a CO unit that is activated toward 1-electron reactions at the carbonyl carbon. This behavior is distinct from other 17-electron d^7 carbonyl complexes which are reported to react exclusively as metal-centered radicals. The acyl radical nature of **4** is shared by 19-electron metal carbonyls,[11-14] but rhodium(II) porphyrins are currently unique in providing an equilibrium source for 1-electron-activated carbon monoxide.

Experimental Section

General Methods. All manipulations were performed under argon or by vacuum techniques. Reagents were purchased from Aldrich or Strem. Research grade carbon monoxide (Matheson) and ^{13}C-labeled carbon monoxide (Aldrich) were used without further purification. Benzene and toluene solvents used in the EPR and NMR studies were first degassed by freeze–pump–thaw cycles and then refluxed over sodium benzophenone until the indicator turned purple. Methylcyclohexane was degassed by freeze–pump–thaw cycles and stored over Linde 4-Å molecular sieves.

NMR Studies. Proton NMR spectra were obtained on a Bruker WP200SY interfaced to an Aspect 300 computer. Carbon-13 spectra were obtained on a Bruker AF500 instrument equipped with a ^{13}C probe. Variable-temperature NMR work was performed with the use of an FTS refrigerator unit (220–280 K) or with the boil-off from liquid nitrogen (below 220 K). Temperature calibration was obtained by using methanol or ethylene glycol as an external standard.

EPR Studies. Electron paramagnetic resonance spectra were obtained by use of an EPR 100 D X-band spectrometer. Temperature measurements were calibrated with a Bruker Model VT unit using N_2 as the cooling source (206–290 K). Isotropic spectra for (TMP)RhCO were obtained at temperatures above 233 K under equilibrium conditions. Anisotropic EPR spectra for (TMP)RhCO were obtained by adding CO to samples containing $(TMP)Rh^{\bullet}$ at 195 K and quickly freezing to 90 K.

Temperature dependence of the relative EPR spectral intensity for toluene solutions of (TMP)RhCO (**4**) have been analyzed to evaluate the enthalpy of dimerization (ΔH°_2). The intensity of the isotropic spectrum for **4** becomes independent of CO pressure when P_{CO} is greater than 0.2 atm, which indicates that virtually all of the $(TMP)Rh^{\bullet}$ is converted to an equilibrium distribution of **4** and **5**. As the temperature is lowered, the EPR intensity of **4** decreases due to formation of **5**. The equilibrium constant expression for reaction 2 is $K_2 = [\mathbf{5}]/[\mathbf{4}]^2 = ([\mathbf{5}]_0 - {}^1/_2[\mathbf{4}])/[\mathbf{4}]^2$. In this reaction, $[\mathbf{4}] \ll [\mathbf{5}]$ and K_2 simplifies ($K_2 \cong [\mathbf{5}]_0/[\mathbf{4}]^2$) where $[\mathbf{5}]_0 = [\mathbf{5}] + {}^1/_2[\mathbf{4}]$ = constant. The EPR spectral intensity for **4** adjusted for the temperature dependence of the spin populations ($I_{(2)}$) is proportional to the molar concentration of **4** ($[\mathbf{4}] = CI_{(4)}$); $K_2 = [\mathbf{5}]_0/C^2I_{(4)}^2 = C'I_{(4)}^{-2}$; $\ln K_2 = -2 \ln I_{(4)} + \ln (C')$. For a single sample examined at different temperatures, the slope of the linear relationship between $-2 \ln I_{(4)}$ and $1/T$ yields $-\Delta H^{\circ}_2/R$ ($\Delta H^{\circ}_2 = -18.3 \pm 0.8$ kcal mol^{-1}) (Figure 3).

Synthesis of (TMP)RhI. In a three-neck flask fitted with an addition funnel and reflux condenser were added dropwise 250 mg of $[Rh(CO)_2Cl]_2$ dissolved in 40 mL of dry 1,2-dichloroethane under argon to a suspension containing 375 mg of $(TMP)H_2$ and 300 mg of anhydrous sodium acetate in 200 mL of 1,2-dichloroethane. The resulting solution mixture was then refluxed under argon for 48 h. After the mixture was cooled to room temperature, I_2 was added in two stages, 100 mg initially and an additional 80 mg after 2 h. The reaction mixture was then stirred at room temperature for an additional 3 h. The crude product was concentrated by rotary evaporation after filtration to remove the inorganic salts and chromatographed on grade 3 alumina using chloroform as the eluent to give the (TMP)RhI in an overall yield of 50–70%: ^1H NMR (C_6D_6) δ 8.83 (s, 8 H, pyrrole H), 2.32 (s, 12 H, *o*-CH_3), 1.75 (s, 12 H, *o'*-CH_3), 7.22 (s, 4 H, *m*-H), 7.05 (s, 4 H, *m'*-H), 2.43 (s, 12 H, *p*-CH_3); FAB MS, m/e = 1010.

$(TMP)RhCH_3$. Ethanol (25 mL) and (TMP)RhI (50 mg) were mixed, and the resultant mixture was warmed to 60 °C for 40 min. The resulting solution was then filtered and the filtrate flushed with argon for 30 min. Addition of 7 mg of $NaBH_4$ in 2 mL of aqueous 0.5 M NaOH to the solution under argon caused a color change from red to yellow-brown, indicating the formation of $(TMP)Rh^{I}$ anion. The resulting solution was then stirred for 30 min. Addition of 0.1 mL of CH_3I resulted in formation of a precipitate which was collected by filtration and identified as $(TMP)RhCH_3$ by ^1H NMR and FAB mass spectra: ^1H NMR (C_6D_6) δ 8.75 (s, 8 H, pyrrole H), 2.26 (s, 12 H, *o*-CH_3), 1.75 (s, 12 H, *o'*-CH_3), 7.20 (s, 4 H, *m*-H), 7.07 (s, 4 H, *m'*-H), 2.43 (s, 12 H, *p*-CH_3), −5.25 (d, 3 H, methyl), $^2J_{^{103}Rh-CH_3} = 2.90$ Hz; FAB MS, m/e = 898.

(TMP)RhH. The hydride complex was prepared using a method similar to that used in the preparation of $(TMP)RhCH_3$ except that acetic acid was added to the $(TMP)Rh^{I}$ anion solution: ^1H NMR (C_6D_6) δ 8.77 (s, 8 H, pyrrole H), 2.14 (s, 12 H, *o*-CH_3), 1.79 (s, 12 H, *o'*-CH_3), 7.03 (s, 4 H, *m*-H), 6.95 (s, 4 H, *m'*-H), 2.43 (s, 12 H, *p*-CH_3), −39.99 (d, 1 H, hydride), $J_{^{103}Rh-H} = 44$ Hz; IR (Nujol) $\nu_{Rh-H} = 2095$ cm^{-1}; FAB MS, m/e = 884.

$(TMP)Rh^{\bullet}$. Samples of $(TMP)Rh^{\bullet}$ for reactivity and physical studies were prepared by photolysis of $(TMP)RhCH_3$. Degassed benzene solutions of $(TMP)RhCH_3$ (0.5–0.8 mg/0.3 mL) in vacuum-adapted NMR or EPR tubes were photolyzed ($\lambda > 350$ nm) for 6 h in a Rayonet photoreactor. The benzene solvent along with the methane and toluene reaction products were removed under vacuum, and dried degassed benzene or toluene solvent was vacuum distilled into the tubes. $(TMP)Rh^{\bullet}$ was identified in solution by the characteristic ^1H NMR and EPR spectra and FAB mass spectra: ^1H NMR (C_6D_6, 296 K) δ 18.3 (broad, 8 H, pyrrole H), 3.35 (broad, 8 H, *o*-CH_3), 8.87 (broad, 8 H, *m*-CH_3), 3.51 (s, 12 H, *p*-CH_3); EPR (toluene glass at 90 K) $g_{\perp} = 2.65$,

$g_{\parallel} = 1.915$, $A_{\perp} = -197$ MHz, $A_{\parallel} = -158$ MHz; UV-vis (C_6H_6) λ_{max} = 412, 522 nm; FAB MS, m/e = 883.

(TMP)RhC(O)C(O)Rh(TMP). Exposure of NMR samples containing (TMP)Rh• in benzene or toluene to carbon monoxide ($P_{CO} > 300$ Torr) results in the formation of (TMP)RhC(O)C(O)Rh(TMP). The ^{1}H NMR spectrum for (TMP)RhC(O)C(O)Rh(TMP) displays broad resonances at room temperature due to exchange with (TMP)RhCO, but the NMR peaks sharpen as the temperature is lowered: ^{1}H NMR (C_6D_6, 280 K) δ 8.32 (s, 16 H, pyrrole H), 1.93 (s, 24 H, *o*-CH_3), 1.17 (s, 24 H, *o'*-CH_3), 2.42 (s, 24 H, *p*-CH_3), *m*-H obscured by the solvent; ^{13}C NMR (toluene-d_8, 193 K) δ 164.9 (AA'XX' m, 2 ^{13}C, Rh^{13}C(O)^{13}C(O)Rh), six transitions observed at ±12, ±17, and ±25 Hz relative to the center of δ 164.9; IR (Nujol mull) ν_{CO} 1782, 1770 cm^{-1}).

(TMP)RhCHO. Benzene solutions of (TMP)Rh• in contact with CO/H_2 mixtures react to form an equilibrium distribution of (TMP)RhCO and (TMP)RhC(O)C(O)Rh(TMP) which then slowly further react with H_2 to produce the formyl complex, (TMP)RhCHO (**4**). When the initial partial pressure of CO exceeds 0.4 atm ($P_{H_2} > 0.2$ atm; T = 296 K), (TMP)RhCHO is the exclusive product observed by ^{1}H NMR. At lower CO pressures ($P_{CO} < 0.3$ atm) where significant amounts of (TMP)Rh• (**1**) persist in the equilibrium distribution, **1** reacts with H_2 to form (TMP)RhH which results in a solution containing ^{1}H observable quantities of **1** and **4**. Independently prepared benzene solutions containing (TMP)RhH or (TMP)RhH and (TMP)Rh• failed to react with CO to produce the formyl complex, **4**. (TMP)RhCHO was identified in solution by ^{1}H and ^{13}C NMR: ^{1}H NMR (C_6D_6) δ 8.81 (s, 8 H, pyrrole H), 3.78 (d, 1 H, RhC*H*O), 2.42 (s, 12 H, *p*-CH_3), 2.21 (s, 12 H, *o*-CH_3), 1.74 (s, 12 H, *o*-CH_3), $^1J_{^{103}Rh-^{13}C}$ = 30.5 Hz, $^1J_{^{13}C-H}$ = 196.5 Hz, $^2J_{^{103}Rh-CHO}$ = 2.0 Hz; IR ν_{CO} 1710, 1733 cm^{-1}.

(TMP)RhC(O)CH$_2$CH(C$_6$H$_5$)C(O)Rh(TMP). A benzene solution of (TMP)Rh radical (10^{-3} M) was pressurized with carbon monoxide ($P_{CO} \cong 400$ Torr) to form an equilibrium distribution of (TMP)RhC(O)C(O)Rh(TMP) and (TMP)RhCO. The sample was then frozen (78 K) and CO removed under vacuum. A 3-fold excess of styrene was added to the frozen sample which was then repressurized with 400 Torr of carbon monoxide. Formation of the four carbon-bridged product reaches completion within 1 day: ^{1}H NMR (C_6D_6) δ 8.49 (d, 4 H, pyrrole H, $^3J_{H-H}$ = 4.5 Hz), 8.47 (d, 4 H, pyrrole H, $^3J_{H-H}$ = 4.5 Hz), 8.47 (d, 4 H, pyrrole H, $^3J_{H-H}$ = 4.5 Hz), 8.43 (d, 4 H, pyrrole, $^3J_{H-H}$ = 4.5 Hz), 6.08 (dd, 1 H, phenyl *p*-H), 5.75 (dd, 2 H, phenyl *m*-H), 3.02 (d, 2 H, phenyl *o*-H), 2.40 (s, 12 H, mesityl *p*-CH_3), 2.37 (s, 12 H, mesityl *p*-CH_3), 1.76 (s, 12 H, mesityl *o*-CH_3), 1.71 (s, 12 H, mesityl *o*-CH_3), 1.53 (s, 12 H, mesityl *o*-CH_3), 1.29 (s, 12 H, mesityl *o*-CH_3), −2.83 (dd, 1 H, $-CH_{(1)}H_{(2)}CH_{(3)}(C_6H_5)-$, $^2J_{(1)(2)}$ = 10.8 Hz, $^3J_{(1)(3)}$ = 2.6 Hz), −3.98 (dd, 1 H, $-CH_{(1)}H_{(2)}CH_{(3)}(C_6H_5)$, $^3J_{(2)(3)}$ = 18.8 Hz), −4.35 (dd, 1 H, $-CH_{(1)}H_{(2)}CH_{(3)}(C_6H_5)-$). The two sets of porphyrin resonances are due to the nonsymmetrical bridging structure. The optically active $-CH(C_6H_5)-$ carbon center results in chemically inequivalent adjacent pyrrole hydrogens which produces an AB coupling pattern for the pyrrole hydrogens. The absence of ^{103}Rh coupling on any of the $-CH_2CH(C_6H_5)-$ alkyl bridge hydrogens indicates that one carbon monoxide is inserted between the styrene and the rhodium atoms on both sides. The reaction was also performed with ^{13}C-enriched carbon monoxide. The ^{1}H NMR of this complex differs from that of the ^{12}CO-containing compound only in the appearance of additional ^{13}C–H coupling on the three highfield alkyl bridge hydrogens ($^2J_{^{13}CH(1)}$ = 4.6 Hz; $^2J_{^{13}CH(2)}$ = 4.8 Hz; $^2J_{^{13}CH(3)}$ = 6.5 Hz). Confirmation of the structure comes from the ^{1}H-decoupled ^{13}C NMR which show two carbonyl ^{13}C resonances with one-bond ^{103}Rh–^{13}C couplings: (C_6D_6) δ 193.40 ($^1J_{^{103}Rh^{13}C}$ = 36 Hz), 196.5 ($^1J_{^{103}Rh^{13}C}$ = 31 Hz).

2,4,6-Triisopropylbenzaldehyde. The general procedure for the synthesis of mesitaldehyde was followed in the preparation of 2,4,6-triisopropylbenzaldehyde.[38] 1,3,5-Triisopropylbenzene (15.0 g, 62.5 mmol) was dissolved in dry methylene chloride (150 mL) in a 250-mL three-necked flask equipped with a reflux condenser, dropping funnel, and syringe input port. The solution was cooled in an ice bath under nitrogen with constant stirring for 20 min, after which time titanium tetrachloride (23.0 mL, 209.1 mmol) was carefully syringed into the flask over a period of 3 min. Dichloromethyl methyl ether (11.8 mL, 130.4 mmol) was then added dropwise via the addition funnel. Dropwise addition of the ether was immediately accompanied by evolution of hydrogen chloride gas as the reaction commenced, and the mixture undergoes a series of color changes (colorless to yellow, then orange, then deep red) during the 25-min addition. The reaction mixture was stirred overnight at room temperature, and the product was vacuum distilled and stored under nitrogen: yield >80%; ^{1}H NMR ($CDCl_3$) δ 10.59 (s, 1 H, −C*H*O), 7.05 (s, 2 H, arom), 3.54 (septet, 2 H, −C*H*−), 2.86 (septet, 1 H, −CH−), 1.21 (d, 18 H, $-CH_3$).

(38) Rieche, A.; Gross, H.; Höft, E. *Org. Synth.* **1967**, *47*, 1.

Tetrakis(2,4,6-triisopropylphenyl)porphyrin, (TTiPP)H$_2$. The porphyrin free base ligand was prepared according to the method developed by Lindsey.[39] 2,4,6-Triisopropylbenzaldehyde (2.32 g, 10 mmol) and a stoichiometric quantity of pyrrole (694 mL, 10 mmol) were dissolved in 1 L of freshly distilled chloroform in an inert atmosphere. BF_3 etherate (1.32 mL, 3.3 mmol) was added as a catalyst, and the reaction proceeded via numerous color changes (colorless, yellow, orange, deep red) prior to formation of a dark green solution. The progression of the reaction was monitored every 15 min by UV-vis absorption spectroscopy.[39] (The initial cyclized product is the tetrakis(triisopropylphenyl)porphyrinogen, which can be oxidized to yield the porphyrin. Hence, each 50-mL aliquot withdrawn from the reaction mixture was oxidized with excess *p*-chloranil prior to evaluation by UV-vis spectroscopy. Porphyrins are recognizable by a characteristic absorption, the Soret band, at $\lambda \approx 420$ nm. The polypyrrylmethane side products are converted to polypyrrylmethenes by the *p*-chloranil oxidation and absorb at higher wavelengths 470–480 nm. The optimum time required to maximize the cyclized porphyrinogen was 90 min. At this time, an excess of *p*-chloranil was added to the reaction mixture and the solution was brought to a gentle reflux (~60 °C) for 1 h. After rotary evaporation, purification of the porphyrin involved chromatographing the crude product on alumina with methanol. The porphyrin is insoluble in methanol and remains on top of the column as a solid. Several washings with methanol were required to remove most of the polypyrrylmethenes, although this occurred with some loss of product. Further purification required cutting out the top portion of the column, dissolving in chloroform, and rechromatographing with chloroform as the eluent. The solvent was then removed by rotary evaporation, the solid dissolved in toluene, and the final purification achieved by chromatography using toluene as the eluent. The complex eluted as a red band on the column. The yield on each synthesis was ~20 mg (~1% yield): ^{1}H NMR (C_6D_6) δ 8.58 (s, 8 H, pyrrole H), 7.50 (s, 8 H, arom), 3.1 (septet, 4 H, −CH−), 2.43 (septet, 8 H, −CH−), 1.51 (d, 24 H, $-CH_3$), 0.98 (d, 48 H, $-CH_3$), −1.61 (broad s, 2 H, −NH); UV-vis ($CHCl_3$) λ_{max} 422, 530 nm; FAB MS, m/e = 1120.

(TTiPP)RhI. To 50 mg of (TTiPP)H$_2$ in 50 mL of chloroform was added dropwise 50 mg of [Rh(CO)$_2$Cl]$_2$ in 25 mL of chloroform under argon. The reaction was allowed to proceed for 36 h whereupon the reaction mixture was brought to room temperature and reacted with 100 mg of iodine. After an additional 2 h, a further 80 mg of iodine was added and the reaction mixture stirred for 3 h more at 25 °C. The resulting solution was filtered to remove inorganic salts and the precipitate washed with copious amounts of fresh chloroform. The organic-soluble fractions were combined, and this crude product was concentrated by rotary evaporation and chromatographed on grade 3 alumina using chloroform as the eluent. The chromatographic procedure was often inefficient because the iodo compound streaks on the column. In such cases, the pure compound could be obtained by first converting to the methyl derivative (vide infra), which is easier to purify by column chromatography, and then converting back by addition of I_2: ^{1}H NMR (C_6D_6) δ 8.59 (s, 8 H, pyrrole H), 7.59 (s, 4 H, arom), 7.45 (s, 4 H, arom), 3.40 (septet, 4 H, $-CH(CH_3)_2$), 3.15 (septet, 4 H, $-CH(CH_3)_2$), 1.94 (septet, 4 H, $-CH(CH_3)_2$), 1.52 (d, 24 H, $-CH(CH_3)_2$), 1.30 (d, 24 H, $-CH(CH_3)_2$), 8.20 (d, 24 H, $-CH(CH_3)_2$); UV-vis ($CHCl_3$) λ_{max} 418, 534 nm; FAB MS, m/e = 1347.

(TTiPP)RhCH$_3$. A 100-mg sample of (TTiPP)RhI (0.07 mmol) was dissolved in 40 mL of ethanol by stirring at 60 °C for 40 min. The resulting deep red solution was filtered in air into a two-neck round-bottom flask and the filtrate flushed with argon for 30 min. Addition of a 3–4-fold excess of $NaBH_4$ (10 mg, 0.27 mmol) in 3 mL of aqueous 0.05 M NaOH to the solution under argon effected a color change from deep red to dark brown, indicating the formation of the (TTiPP)Rh$^-$ anion. The resulting solution was then stirred for 30 min. Addition of 0.15 mL of CH_3I (2.4 mmol) resulted in the formation of (TTiPP)Rh-CH_3 as a light orange precipitate, which was collected by filtration. After the precipitate was dried for 2 h, ^{1}H NMR was used to determine the purity of the product. Column chromatography on grade 3 alumina ($CHCH_3$ eluent) was used to purify the compound if necessary: ^{1}H NMR (C_6D_6) δ 8.52 (s, 8 H, pyrrole H), 7.58 (s, 4 H, arom), 7.45 (s, 4 H, arom), 3.16 (septet, 8 H, $-CH(CH_3)_2$), 2.01 (septet, 4 H, $-CH(CH_3)_2$), 1.51 (d, 24 H, $-CH(CH_3)_2$, 1.25 (d, 24 H, $-CH(CH_3)_2$), 0.85 (d, 24 H, $-CH(CH_3)_2$), −5.50 (d, 3 H, RhCH_3, $^2J_{Rh-CH_3}$ = 3.2 Hz).

Synthesis of (TTiPP)RhI from (TTiPP)RhCH$_3$. A 3-fold excess of iodine was added to the metalloalkyl complex in chloroform. The reaction was allowed to proceed overnight. Removal of the solvent resulted in isolation of a green paramagnetic compound formulated as

(39) (a) Wagner, R. W.; Lawrence, D. S.; Lindsey, J. S. *Tetrahedron Lett.* **1987**, *28*, 3069. (b) Lindsey, J. S.; Hsu, H. C.; Scheiman, I. C. *Tetrahedron Lett.* **1986**, *27*, 4969. (c) Lindsey, J. S.; Schreiman, I. C.; Hsu, H. C.; Kearney, P. C.; Marguerettaz, A. M. *J. Org. Chem.* **1987**, *52*, 827.

$(TTiPP^+)Rh(I)_2^-$. This compound was then washed twice with a sodium thiosulfate solution for removal of excess iodine and then with water. The final product (TTiPP)RhI, was then dissolved in chloroform and dried with anhydrous $MgSO_4$.

(TTiPP)Rh•. Photolysis of (TTiPP)$RhCH_3$ in benzene produced the metalloradical, (TTiPP)Rh•, at ambient temperature. Clean conversion of (TTiPP)$RhCH_3$ to the metallo radical species was obtained by irradiation of 1-mg samples of (TTiPP)$RhCH_3$ in 0.5 mL of benzene for ~6 h ($\lambda \geq 350$ nm):

$$2(TTiPP)RhCH_3 + C_6D_6 \rightarrow 2(TTiPP)Rh^\bullet + CH_3D + C_6D_5CH_3$$

^1H NMR (C_6D_6, 298 K) δ 18.4 (broad, 8 H, pyrrole H), 9.19 (broad, 8 H, arom), 4.19 (broad, 12 H, $-CH(CH_3)_2$), 2.38 (broad, 24 H, $-CH(CH_3)_2$), 1.53 (broad, 48 H, $-CH(CH_3)_2$).

(TTiPP)RhCO. Exposure of NMR samples containing (TTiPP)Rh• in benzene or toluene to carbon monoxide ($P_{CO} > 100$ Torr) resulted in the formation of (TTiPP)RhCO. The ^1H NMR spectrum for (TTiPP)RhCO displays broad contact shifted resonances at room temperature. No diamagnetic products were observed: ^1H NMR (C_6D_6, 298 K, 450 Torr of CO) δ 18.0 (broad, 8 H, pyrrole H), 9.15 (broad, 8 H, arom), 4.05 (broad, 12 H, $-CH(CH_3)_2$), 2.254 (broad, 24 H, $-CH(CH_3)_2$), 1.50 (broad, 48 H, $-CH(CH_3)_2$).

Addition of ^{13}CO to a toluene solution of (TTiPP)Rh• produced (TTiPP)$Rh^{13}CO$ which displays an isotropic EPR spectrum ($\langle g \rangle = 2.10$, $\langle A(^{13}C) \rangle = 320$ MHz). Frozen toluene solutions (90 K) display three distinct g values and ^{13}C coupling constants associated with a nonlinear RhCO unit ($g_1 = 2.167$; $g_2 = 2.130$; $g_3 = 2.000$; $A(^{13}C_{(g_1)}) = 318$ MHz; $A(^{13}C_{(g_2)}) = 347$ MHz; $A(^{13}C_{(g_3)}) = 305$ MHz; $A(^{13}C_{(g_3)}) = 65$ MHz). In contrast with (TMP)RhCO, lowering the temperature from 283 to 233 K resulted in a regular increase in the intensity of the isotropic EPR of (TTiPP)RhCO.

Acknowledgment. This work was supported by the National Science Foundation and the Department of Energy, Division of Chemical Sciences, Office of Basic Energy Sciences, Grant DE-FG02-86ER13615.

Spin Exchange Coupling in Asymmetric Heterodinuclear Complexes Containing the μ-Oxo-bis(μ-acetato)dimetal Core

Rainer Hotzelmann,[1a] Karl Wieghardt,*[,1a] Ulrich Flörke,[1b] Hans-Jürgen Haupt,[1b] David C. Weatherburn,[1c] Jacques Bonvoisin,[‡,1d] Geneviève Blondin,[1d] and Jean-Jacques Girerd*[,1d]

Contribution from the Lehrstuhl für Anorganische Chemie I, Ruhr-Universität, D-4630 Bochum, FRG, the Lehrstuhl für Allgemeine Anorganische und Analytische Chemie der Universität-Gesamthochschule, D-4790 Paderborn, FRG, Department of Chemistry, Victoria University of Wellington, P.O. Box 600, Wellington, New Zealand, and Laboratoire de Chimie Inorganique, Institut de Chimie Moléculaire d'Orsay, Université de Paris-Sud, F-91405 Orsay, France. *Received June 20, 1991*

Abstract: Synthesis of asymmetric *hetero*dinuclear complexes $[LM^1(\mu\text{-}O)(\mu\text{-}CH_3CO_2)_2M^2L']^{2+}$, where L represents 1,4,7-triazacyclononane, L' is 1,4,7-trimethyl-1,4,7-triazacyclononane, and M^1 and M^2 are two different trivalent first-row transition metals, has been achieved by the hydrolytic reaction of an equimolar mixture of LM^1Cl_3 and $L'M^2Cl_3$ in aqueous sodium acetate solution. The asymmetric *homo*dinuclear species $[LM(\mu\text{-}O)(\mu\text{-}CH_3CO_2)_2ML']^{2+}$ (M = Mn^{III} (**1**), Fe^{III} (**2**)) have also been prepared. The following heterodinuclear species have been isolated as PF_6^- or ClO_4^- salts and characterized: $Fe^{III}Mn^{III}$ (**3**), $Fe^{III}Cr^{III}$ (**4**), $Cr^{III}Mn^{III}$ (**5**), and $Cr^{III}V^{III}$ (**7**). **4** is protonated in acidic solution affording the μ-hydroxo bridged complex $[L'Cr(\mu\text{-}OH)(\mu\text{-}CH_3CO_2)_2FeL](ClO_4)_3 \cdot 2H_2O$ (**4H**). Oxidation of **3** and **5** in aqueous solution with $Na_2S_2O_8$ gave $[L'Fe^{III}(\mu\text{-}O)(\mu\text{-}CH_3CO_2)_2Mn^{IV}L](ClO_4)_3 \cdot H_2O$ (**8**) and $[L'Cr^{III}(\mu\text{-}O)(\mu\text{-}CH_3CO_2)_2Mn^{IV}L](ClO_4)_3$ (**6**). The crystal structures of the ClO_4^- salts of **3**, **5**, and **6** and the PF_6^- salt of **4** have been determined by single crystal X-ray crystallography: **3**, monoclinic $C2/c$, $a = 23.929$ (6) Å, $b = 19.036$ (5) Å, $c = 16.701$ (3) Å, $\beta = 119.52$ (1)°, $Z = 8$; **4**, orthorhombic $Pbca$, $a = 18.951$ (4) Å, $b = 14.160$ (5) Å, $c = 24.619$ (5) Å, $Z = 8$; **5**, monoclinic $P2_1/c$, $a = 11.146$ (2) Å, $b = 20.975$ (4) Å, $c = 13.563$ (3) Å, $\beta = 99.71$ (2)°, $Z = 4$. **6**, monoclinic $P2_1/m$, $a = 11.332$ (3) Å, $b = 9.715$ (1) Å, $c = 16.180$ (4) Å, $\beta = 110.16$ (1)°, $Z = 2$. Bulk magnetic properties of all compounds have been studied in the temperature range 4.2-298 K. It has been found that the spins of the two paramagnetic metal ions are either intramolecularly antiferromagnetically (**2**, **3**, **4**, **4H**, **6**, **8**) or ferromagnetically coupled (**1**, **5**, **7**). An analysis of the interacting magnetic orbitals in complexes containing the μ-oxo-bis(μ-carboxylato)dimetal core is presented.

Introduction

Electronic and magnetic properties of dinuclear oxo-bridged iron proteins have in the past two decades received the attention of biochemists, inorganic chemists, and physicists.[2] This class of non-heme metalloproteins contains, as a common structural feature in their fully oxidized forms, two high-spin ferric ions which are bridged by one oxo ligand and, in addition, by one or two carboxylates. Structurally characterized examples are azidomethemerythrin,[3] hemerythrin, and, very recently, ribonucleotide reductase[4] all of which contain a bent Fe^{III}–O–Fe^{III} moiety. Other metalloproteins which are believed to contain this unit in its ferric form are the purple acid phosphatases[5] and uteroferrin. In all cases a strong antiferromagnetic coupling of the unpaired spins

‡Present address: CEMES LOE, UPR A 8011, BP 4347, 29, Rue Jeanne Marvig, F-31055 Toulouse, France.

(1) (a) Ruhr-Universität Bochum. (b) Universität Paderborn. (c) Victoria University of Wellington. (d) Université de Paris-Sud.

(2) (a) Lippard, S. J. *Angew. Chem., Int. Ed. Engl.* **1988**, *27*, 344. (b) Sanders-Loehr, J. In *Physical Bioinorganic Chemistry 5: Iron Carriers and Iron Proteins*; Loehr, T. M., Ed.; VCH Publishers: New York, Weinheim, Cambridge, 1989; p 373. (c) Kurtz, D. M., Jr. *Chem. Rev.* **1990**, *90*, 585. (e) Que, L., Jr.; True, A. E. *Progr. Inorg. Chem.* **1990**, *38*, 97.

(3) (a) Stenkamp, R. E.; Sieker, L. C.; Jensen, L. H. *J. Am. Chem. Soc.* **1984**, *106*, 618. (b) Sieker, L. C.; Stenkamp, R. E.; Jensen, L. H. In *The Biological Chemistry of Iron*; Dunford, H. B., Dolphin, D., Raymond, K. N., Sieker, L. C., Eds.; D. Reidel Publishing Company: Boston, MA, 1982; p 161. (c) Holmes, M. A.; Trong, I. L.; Turley, S.; Sieker, L. C.; Stenkamp, R. E. *J. Mol. Biol.* **1991**, *218*, 583.

0002-7863/92/1514-1681$03.00/0